Theor Chim Acta (1987) 72: 265-276

Theoretica Chimica Acta

The use of supercomputers for the variational calculation of ro-vibrationally excited states of floppy molecules*

Brian T. Sutcliffe[1], Jonathan Tennyson[2] and Steven Miller[2]

[1] Department of Chemistry, University of York, York Y01 5DD, UK
[2] Department of Physics and Astronomy, University College London, Gower Street, London WC1E 6BT, UK

The advent of supercomputers has led to great advances in electronic structure calculations and to the *ab initio* calculation of molecular spectra. Recent theoretical developments have allowed us to develop a two-step variational algorithm for the calculation of rotationally highly excited states of floppy molecules. This algorithm allows highly accurate nuclear motion calculations to be performed on low-lying ro-vibrational states and greatly extends the range of states that can practicably be considered. The algorithm has been adapted to run efficiently on the Cray supercomputers. Analysis of the timings suggest that construction of the secular matrix is highly vectorised and that the special structure of secular matrix can be used to give rapid diagonalisation. The limiting factor on these calculations is the available fast storage, but analysis suggests that this bottleneck could be removed by use of a Solid State Device (SSD). Sample results are given for calculations involving a range of rotational excitation. An adaptation of the algorithm to a loop of parallel processors is also suggested.

Key words: Vibration-rotation — Variational method — Supercomputers — Diagonalisation

1. Introduction

The impact of supercomputers on molecular structure calculations has been a profound one and is directly discussed in other contributions here. Since their

* This paper was presented at the International Conference on 'The Impact of Supercomputers on Chemistry', held at the University of London, London, UK, 13-16 April 1987

advent it has become possible to calculate in a reasonable time highly accurate electronic energies for sufficient nuclear geometries to enable the construction of high-quality, non-empirical potential energy surfaces for molecules with three or four nuclei and up to ten electrons. Such surfaces make feasible completely non-empirical calculations of molecular rotation-vibration spectra, at least within the Born–Oppenheimer approximation, where previously only semi-empirical work was possible. This article is directed to a consideration of a scheme for such calculations on the Cray range of supercomputers. The emphasis of the article is therefore less on new results than on computational techniques.

The calculational scheme presented here arose from a perception that the traditional approach to the problem of rotation-vibration spectra, based on the concept of an equilibrium geometry and near-harmonic vibrations, was likely to be inapplicable to the description of systems in highly excited states performing large amplitude vibrations. Such systems are now experimentally accessible through developments in high resolution laser spectroscopy. It will be shown that the method we use is capable of achieving, at least for H_3^+ and its isotopomers, an accuracy competitive with that achieved by experiment [1, 2]. The magnitude of this achievement is perhaps best appreciated if it is remembered that one is discussing errors in observed ro-vibrational transitions which are six or more orders of magnitude less in energy than the dissociation energy of the molecule. This achievement would not have been possible without access to supercomputers.

The success of these techniques has naturally led to questions about regions of the molecular spectrum as yet not directly sampled by laser spectroscopy. Here accurate calculations are the only possible means of obtaining information. Studies in this area have concentrated on the highly excited states of triatomic species [3–7] and, more recently, on highly rotationally excited states [8, 9]. It is from calculations in the latter problem area that the examples presented here will be chosen.

The theoretical background to the approach used is described in two recent papers [8, 10]. It will simply be summarised to provide the context in which the computational scheme can be understood and the meaning of the results appreciated.

2. Theory

Unlike electronic structure calculations where the Hamiltonian of the problem is well defined, a variety of Hamiltonians and consequent solution techniques are available for the nuclear motion problem. This is because of the need to separate the continuous spectrum due to the translational motion of the system and the desirability of identifying vibrational and rotational coordinates.

Sutcliffe and Tennyson [10] recently derived a Hamiltonian for the nuclear motion of a triatomic in a generalised coordinate system. These coordinates are the distance between atoms 2 and 3, r_1; the distance, r_2, from an arbitrary point on $\boldsymbol{r}_1$ to atom 1, and the angle, θ, between $\boldsymbol{r}_1$ and $\boldsymbol{r}_2$. The Hamiltonian is to be used

in linear variational calculations where the variational basis consists of products of functions of the internal coordinates and standard rotation functions $|J, M, k\rangle$ [10-12]. The purely rotational part of this basis can be integrated out to leave a Hamiltonian which acts upon the functions of the internal coordinates (r_1, r_2, θ). This can be written:

$$\mathcal{H} = \mathcal{K}_V^{(1)} + \mathcal{K}_V^{(2)} + \mathcal{K}_{VR}^{(1)} + \mathcal{K}_{VR}^{(2)} + V(r_1, r_2, \theta) \tag{1}$$

with

$$\mathcal{K}_V^{(1)} = -\delta_{k'k}\frac{\hbar^2}{2}\left[\frac{1}{\mu_1 r_1^2}\left(\frac{\partial}{\partial r_1} r_1^2 \frac{\partial}{\partial r_1} + \frac{1}{\sin\theta}\frac{\partial}{\partial\theta}\sin\theta\frac{\partial}{\partial\theta}\right)\right.$$
$$\left. + \frac{1}{\mu_2 r_2^2}\left(\frac{\partial}{\partial r_2} r_2^2 \frac{\partial}{\partial r_2} + \frac{1}{\sin\theta}\frac{\partial}{\partial\theta}\sin\theta\frac{\partial}{\partial\theta}\right)\right] \tag{2}$$

$$\mathcal{K}_V^{(2)} = \delta_{k'k}\frac{\hbar^2}{\mu_{12}}\left[-\cos\theta\frac{\partial^2}{\partial r_1 \partial r_2} + \frac{\cos\theta}{r_1 r_2}\left(\frac{1}{\sin\theta}\frac{\partial}{\partial\theta}\sin\theta\frac{\partial}{\partial\theta}\right)\right.$$
$$\left. + \sin\theta\left(\frac{1}{r_1}\frac{\partial}{\partial r_2} + \frac{1}{r_2}\frac{\partial}{\partial r_1} + \frac{1}{r_1 r_2}\right)\frac{\partial}{\partial\theta}\right] \tag{3}$$

$$\mathcal{K}_{VR}^{(1)} = \delta_{k'k}\hbar^2\left[\frac{(J(J+1)-2k^2)}{2\mu_1 r_1^2} + \frac{k^2}{2}\operatorname{cosec}^2\theta\left(\frac{1}{\mu_1 r_1^2} + \frac{1}{\mu_2 r_2^2} - \frac{2\cos\theta}{\mu_{12} r_1 r_2}\right)\right]$$
$$+ \delta_{k'k\pm1}\frac{\hbar^2}{2\mu_1 r_1^2} C_{Jk}^{\pm}\left(\mp\frac{\partial}{\partial\theta} + k\cot\theta\right) \tag{4}$$

$$\mathcal{K}_{VR}^{(2)} = \delta_{k'k\pm1}\frac{\hbar^2 C_{Jk}^{\pm}}{2\mu_{12} r_1 r_2}\left(\pm\cos\theta\left(\frac{\partial}{\partial\theta} \mp k\cot\theta\right) \pm \left(r_2\frac{\partial}{\partial r_2} \mp k\right)\sin\theta\right). \tag{5}$$

The effective Hamiltonian (1) is diagonal in the total angular momentum J and independent of its projection onto the laboratory z axis, M. The kronecker deltas show the coupling with in the $(2J+1)$ dimensional rotational manifold with the projection of J onto the body-fixed z axis, $k = -J, -J+1, \ldots 0 \ldots, J-1, J$. The form given above is appropriate for the body-fixed z-axis embedded along $\boldsymbol{r}_1$. The embedding along $\boldsymbol{r}_2$ is obtained simply by making the exchanges $r_1 \leftrightarrow r_2$ and $\mu_1 \leftrightarrow \mu_2$. The coefficients $C_{Jk}^{\pm}$ are the usual step up and down coefficients

$$C_{Jk}^{\pm} = (J(J+1) - k(k\pm1))^{1/2} \tag{6}$$

and the reduced masses are given by

$$\begin{aligned}
\mu_1^{-1} &= m_2^{-1} + m_3^{-1} \\
\mu_{12}^{-1} &= g(m_2^{-1} + m_3^{-1}) - m_3^{-1} \\
\mu_2^{-1} &= m_1^{-1} + g^2 m_2^{-1} + (1-g)^2 m_3^{-1}
\end{aligned} \tag{7}$$

with

$$g = (r_1 - v)/r_1 \tag{8}$$

where v is the distance from atom 2 to the point at which $\boldsymbol{r}_2$ cuts $\boldsymbol{r}_1$. It should be noted that if the origin of $\boldsymbol{r}_2$ is chosen at the centre of diatomic mass then $g = m_2/(m_2+m_3)$ and μ_{12}^{-1} vanishes; the resulting internal coordinates are usually called scattering coordinates.

If one uses Hamiltonian (1) directly to perform fully coupled ro-vibrational calculations, the secular matrix rapidly becomes intractable with increasing total angular momentum, J, since every function of the internal coordinates must in principle be associated with $2J+1$ rotational functions. Actually in the problems considered this increase is not quite so fast as symmetry can be used to give separate problems of dimension $J+p$ with $p=0$ and 1. The parity of these problems is given by $(-1)^{J+p}$. Even so the rapid increase with J has limited calculations of this type to J values of 4 or less. However, for many systems, the projection of J along the body-fixed z-axis, k, is nearly conserved. In this case it is possible to obtain approximate solutions of (1) by neglecting terms off-diagonal in k, the so-called off-diagonal Coriolis interactions, and solving the Hamiltonian:

$$\mathscr{H}_k = \mathscr{K}_V^{(1)} + \mathscr{K}_V^{(2)} + \delta_{k'k}\mathscr{K}_{VR}^{(1)} + V(r_1, r_2, \theta) \tag{9}$$

where $\delta_{k'k}\mathscr{K}_{VR}^{(1)}$ signifies the first term in (4). Solutions of the full problem can then be obtained by expanding the wavefunction in terms of solutions of $\mathscr{H}_k$. This method leads to considerable savings because firstly not all the solutions of $\mathscr{H}_k$ are required to converge the low-lying states of the problem and secondly the resulting secular matrix has a sparse structure which can be utilised computationally.

The linear variational solution with eigenvalue $\varepsilon_{k,i}$ to the problem specified by $\mathscr{H}_k$ can be written

$$|k, i\rangle = \sum_{j,m,n} c_{j,m,n}^{J,k,i} |j, k\rangle |m\rangle |n\rangle |J, M, k\rangle \tag{10}$$

where $|j, k\rangle$ is an associated Legendre polynomial and carries the θ coordinate; $|m\rangle$ and $|n\rangle$ are radial basis functions carrying the r_1 and r_2 coordinates respectively and $|J, M, k\rangle$ is included formally to emphasise that in the present approach the base energies are J dependent. In terms of the functions (10), the matrix elements of the full Hamiltonian (1) are

$$\langle k', i'|\mathscr{H}|k, i\rangle = \delta_{k,k'}\delta_{i,i'}\varepsilon_{k,i} + \delta_{k\pm1,k'}\langle k', i'|\mathscr{K}_{VR}^{(1)} + \mathscr{K}_{VR}^{(2)}|k, i\rangle. \tag{11}$$

The off-diagonal matrix elements over the Coriolis operators (the second term in (11)) can be evaluated using matrix elements of the original basis functions. In turn these matrix elements are evaluated analytically or using Gaussian quadrature. For further details on this and other aspects of the theory the reader is referred to [8, 10, 11]. The whole procedure is available as a program suite [12].

3. Computational considerations

The first step in the two-step variational ro-vibrational calculation is the solution of a series of secular problem specified by the Hamiltonian (9). This is technically the same process as solving a pure, $J=0$, vibrational problem. Very efficient algorithms for obtaining such solutions have been developed [7, 11, 13]. In the present case the centrifugal distortion terms arising from the first part of $\mathscr{K}_{VR}^{(1)}$ effectively modify the pure potential so that it depends on J and k. In the present

case one needs to solve a vibrational problem for each modified potential. For a given J, $J+1$ such vibrational calculations need to be solved as $\mathscr{H}_k$ only contains terms in k^2.

The solution of the vibration-like problem divides into two stages, the construction and then the diagonalisation of the secular matrix. Experience has shown that if sufficient care is taken with the selection and implementation of numerical integration procedures, it is usually possible to construct the secular matrix quicker than one can diagonalise it. How this is done in practice depends on the exact nature of the coordinate system and basis functions used. References [11, 13, 15] give details for particular implementations.

Typically, for a pure vibrational calculation the diagonalisation involves obtaining about the 20 lowest eigenvalues and eigenvectors from a matrix of dimension several hundred. The matrix may be neither sparse nor diagonally dominant. Efficient, vectorised routines are available for this problem [14]. We note that if these eigenvectors are to form the basis for a second variational step, then many more, up to half [2], of them may be required. In this case it may be more efficient to use an algorithm which yields all the eigenvectors of a given matrix.

Sample timings with an earlier version of our code, ATOMDIAT2 [16], have demonstrated that a speed-up by a factor of about 15 is possible between scalar and vector versions of the code on a Cray-1S. To obtain these savings it was necessary to use a vectorised diagonaliser and hence store the secular matrix in full rather than lower triangular form. It was also necessary to restructure the secular matrix construction step which otherwise became rate-determining [11].

Although the second variational step can also be thought of as consisting of the two stages, construction and diagonalisation of the secular matrix, the computational considerations involved are rather different. The matrix elements of the second secular problem involve only one-dimensional quadrature. Actually these matrix elements are composed of integrals already calculated in the first step and so only transformations are involved in their construction. The resulting secular matrix has a characteristic structure which is sparse and special techniques can be used to handle it.

In this case, the secular matrix can be stored as a vector of diagonal elements containing the $\varepsilon_{i,k}$ and a rectangular matrix of off-diagonal elements $\boldsymbol{O}$. If the N lowest eigenfunctions of $\mathscr{H}_k$ are used for each k, then $\boldsymbol{O}^k$ contains the N^2 dimensional block linking $|k, i\rangle$ and $|k+1, i'\rangle$. There are $J-p$ such blocks. The storage requirement is thus approximately a factor J less than that of the entire matrix [2, 11].

If the calculation is performed in scattering coordinates, $g = m_2/(m_2+m_3)$, with z embedded along $\boldsymbol{r}_2$ then $\mathscr{K}^{(2)}_{VR}$ vanishes and $\mathscr{K}^{(1)}_{VR}$ simplifies so that

$$O^k_{i,i'} = C^+_{J,k} \sum_{j,m,n} \sum_{j',m',n'} C^+_{j,k} \delta_{j,j'} \delta_{m,m'} \langle n' | \frac{1}{2\mu_2 r_2^2} | n \rangle \times c^{J,k,i}_{j,m,n} c^{J,k+1,i'}_{j,m,n'}. \tag{12}$$

In (12) the outer sums run over the basis functions of the first step. In a computational implementation the loops over i and i', the N solutions of $\mathcal{H}_k$ and $\mathcal{H}_{k+1}$ respectively, are placed innermost as this gives a vectorisable structure. Although the results presented here concentrate on calculations performed in scattering coordinates, it is worth noting that other coordinate systems, for which $\mathcal{K}_{VR}^{(2)}$ is not a null operator, lead to more complicated forms of Eq. (12). In particular extra loops are introduced as non-zero matrix elements off-diagonal in both j, m and n must be incorporated. Computationally this may lead to a balance between coordinates which are the most physical for a particular system and those for which the most efficient calculations can be performed.

Figures 1 and 2 show the time taken to construct the secular matrix as a function of N. These timings show a very nearly linear increase with N despite the fact that from (12) it is apparent that this process depends on N^2 scalar operations. The figures also show the time taken to diagonalise the secular matrices. The timings are for obtaining the 20 lowest eigenvalues, to a tolerance of 0.01 cm^{-1}, and corresponding eigenvectors. The secular matrices are of dimension $S = (J+1-p) * N$; the largest considered in the figures is of dimension 8400. For the smaller problems considered the diagonalisation time is very similar to the matrix construction time. For the larger problems diagonalisation time displays an N^3 behaviour typical of diagonalisation and thus begins to dominate. However, the CPU time used is still small for the size of matrices under consideration. To achieve this it was necessary to use a diagonalisation procedure specifically adapted to the Cray architecture. This will be discussed below.

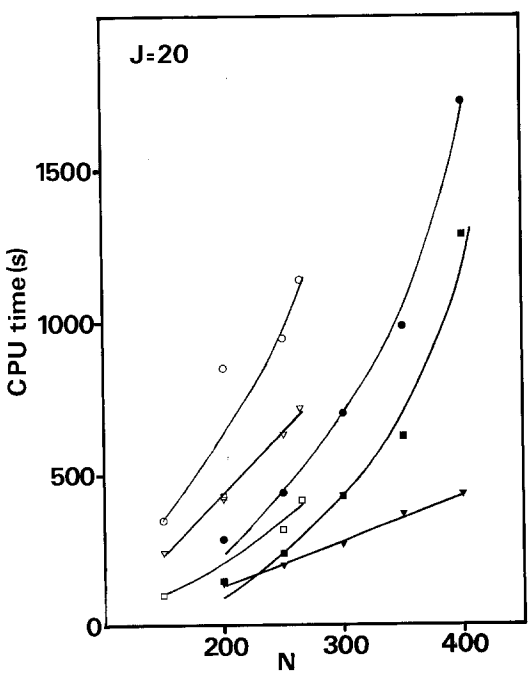

Fig. 1. CPU time usage as a function of N for the second step of a ro-vibrational calculation on H_2D^+ with $J = 20$ ($p = 0$ para). All calculations obtained the lowest 20 levels. The timings are divided into matrix construction (*triangles*) and diagonalisation (*squares*). Total times are given by the *circles*. *Open symbols* are for the Cray-1S/COS2M machine at the University of London Computer Centre and *closed symbols* for the Cray-XMP 480 at the Atlas Computing Centre. For comparison, it took 296s to solve the first step with $N = 100$ on the Cray-1S and 341s to obtain all 1592 solutions of the first step on the Cray-XMP

We have already noted that the secular matrix for the final step of our two-step procedure has a special structure. In order to utilise this structure it is necessary to use an algorithm based on iterative diagonalisation. This not only minimises the storage, but comparisons [8] with diagonalisers designed for symmetric [14] and banded [17] matrices have shown that iterative diagonalisation [18, 19] can also be made faster.

The step characteristic of iterative diagonalisers is the multiplication of the secular matrix by an image vector z:

$$w_l = \sum_{j=1}^{S} H_{lj} z_j \tag{13}$$

The special structure of $\boldsymbol{H}$ means that this operation can be written:

$$w_{k,i} = \varepsilon_{k,i} z_{k,i} + \sum_{i'=1}^{N} (O^k_{i,i'} z_{k+1,i'} + O^{k-1}_{i',i} z_{k-1,i'}) \tag{14}$$

where the symmetry of $\boldsymbol{H}$ has been used implicitly by transposing $\boldsymbol{O}^{k-1}$ in the second product. Computation of $\boldsymbol{w}$ is thus reduced from S vector-matrix multiplications of dimension S to a dot product of dimension S and $2(J-p)$ vector-matrix multiplications of dimension N. For the vector-matrix multiplications we have employed a routine specifically designed for Cray computers [20]. One property of this routine is that it skips the vector-matrix multiplication for zero elements of the vector.

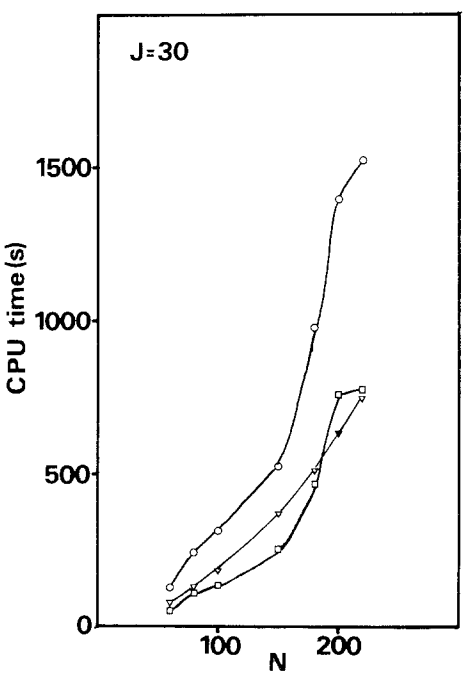

Fig. 2. Cray-1S/COS2M CPU time usage as a function of N for the second step of a ro-vibrational calculation on H_2D^+ with $J = 30$ ($p = 0$ para). All calculations obtained the lowest 20 levels. The timings are divided into matrix construction (▽), diagonalisation (□) and total (○) times. For comparison it took 437s to obtain the solutions of the first step with $N = 100$

For many systems, ones for which k is nearly a good quantum number, the vectors have one dominant coefficient. For example recent calculations on the Ar-CO Van der Waals complex with $J = 1 - 20$ have shown that for the great majority of eigenvectors one solution of $\mathscr{H}_k$ gives more than 90% of the wavefunction [21]. This suggests that unit vectors provide a computationally efficient starting point for the iterations. If T eigenvalues are required, the T lowest diagonal elements are determined prior to diagonalisation and initial guesses are generated as the corresponding unit vectors. At the same time the highest diagonal element is also determined. The diagonals are then shifted so that the highest element takes the value zero. This ensures that only the lowest eigenvalues are determined by a procedure designed to obtain the T eigenvalues with largest absolute value.

Analysis of the diagonalisation times given in Figs. 1 and 2 show that for large N the increase is roughly proportional to N^3, but that this behaviour is far from monotonic. The key to this bumpiness is the number of iterations required to achieve convergence. This number is found to rise approximately linearly with N, but not smoothly so. The cause of this bumpiness remains unclear. Convergence can be affected by the choice of starting vectors, but these are the same for different N. Another possible explanation is that in certain cases there are accidental near-degeneracies [18]. However, analysis of the $J = 20$, $N = 200$ example in Fig. 1, which has the most anomalously long diagonalisation time, gives no evidence to support this explanation. Indeed the $J = 20$, $N = 250$ case, which takes less time to diagonalise actually has two pairs of levels much closer than any in the $N = 200$ case. When the diagonalisation time is divided by the number of iterations, it is found that the time per iteration is proportional to N^2, as would be expected from the structure of Eq. (14).

Table 1. Comparison of CPU time usage (in seconds) and fast memory (in words) for obtaining the lowest 20 ro-vibrational levels of H_2D^+ with $J = 2$ ($p = 0$ para). All calculations yielded the same eigenvalues to within 0.02 cm^{-1} at most. The timings are divided into secular matrix construction (C) and diagonalisation (D) times. All calculations were based on program TRIATOM [12] with the lowest 600 $k = 0$ basis functions preselected on energy ordering grounds [2, 11]. S_{max} gives the dimension of the largest secular matrix in each step of the calculation

	One-step calculation	Two-step calculation		
Cray computer	XMP 480	XMP 480	XMP 480	1S/COS1M
First step				
S_{max}	1 592	600	600	600
Storage/words	2 715 613	536 189	536 189	717 533
t_C/s	2.25	2.15	2.15	4.07
t_D/s	261.78	35.14	35.09	58.36
Second step				
S_{max}		1 592	900	900
Storage/words		1 268 878	544 570	546 370
t_C/s		145.78	23.04	81.50
t_D/s		18.44	7.38	20.11
Total time/s	264.03	201.51	67.66	164.04

A comparison that can be made from Fig. 1 and also Table 1 concerns the relative speed of the codes on the Cray-1S and Cray-XMP machines. For construction of the secular matrix in the second variational step, we find that the XMP is more than three times faster than the 1S machine. This is more than twice the speed-up one would expect simply from the clock speed and implies that additional speed is being gained from vectorisation. For the diagonalisation step time savings are less and also more erratic, varying from about 1.2 to 3 times as fast. The net result is that for the larger runs considered the diagonalisation time dominates on the Cray-XMP.

The memory requirement for the calculations presented in Figs. 1 and 2 increases linearly with J and quadratically with N. The requirement of the largest shown ($J=20$, $N=400$) is approximately 4 Mwords. It is easy to envisage a situation where random access memory is a serious constraint on the size of problem that can be considered. In this respect it should be noted that the algorithm implied by (14) only requires one block of $\boldsymbol{O}$ to be retained in random access memory at a time. This suggests that the procedure can be further adapted to systems such as the Cray XMP 480 newly installed at the Atlas Computing Centre which has a very fast input/output link to a Solid State Storage Device.

4. Sample results

The advent of super-computers has opened up a new era in the *ab initio* calculation of molecular vibration-rotation spectra. Such computers have made possible rapid and accurate calculation of electronic energies for systems with few electrons. In consequence, accurate potential energy surfaces for significant molecular systems are now available. For example the molecular ion H_3^+ has excited much recent interest [22, 23].

Another consequence of these developments has made it possible to transcend the usual semi-rigid approximations used previously in vibration-rotation calculations. This has opened up to theory previously inaccessible spectral regions of great experimental interest. Current work on the near-dissociation spectrum of H_3^+ neatly illustrates that in some important cases it is no longer our ability to perform electronic structure calculations that needs to be improved, but our representation of bound state nuclear dynamics [24]. In this section we briefly illustrate the results which are obtainable with the procedures discussed above.

Table 1 illustrates the computational requirements of several calculations using the algorithms discussed above. The calculations are for a case of low rotational excitation, $J=2$, but clearly illustrate the savings of using our two-step procedure for a calculation. The results presented are for highly converged calculations in which none of the corresponding eigenvalues differed from each other by more than 0.02 cm^{-1}. In the first two calculations presented, the full 1592 dimensional secular matrix was diagonalised. In the first calculation this was done directly; in the second, two steps were used but all the intermediate functions were included in the final calculations. The results of these two procedures are identical within the tolerance of the iterative diagonaliser (here set at 0.01 cm^{-1}). Clearly, the

two-step procedure is not only quicker, but requires less than half the storage of the one-step calculation. The third calculation shows that these savings are greatly increased if only the lowest 300 solutions of $\mathscr{H}_k$ are used in the second step. The final column reports the characteristics of such a calculation on the Cray-1S. Note that the difference in core usage in the first step is due to the use of different diagonalisers.

Table 2 compares rotation-vibration levels for D_2H^+ with $J \leq 4$. The comparison between the most recent theoretical predictions and experiment are excellent. The improvement in the theoretical results over the previous *ab initio* estimates can be ascribed to two effects. Firstly the electronic potential used, due to Meyer et al. [22], which is the most accurate currently available. Secondly, the algorithms discussed above have greatly improved the accuracy of calculations on rotationally excited states. This is particularly true when these states are associated with simultaneous vibrational excitation. We note one advantage of theory over observation is that is allows a complete determination of all the levels, including those of bands which have yet to be characterised experimentally. Further details of these calculations, as well as fits to experimentally motivated model Hamiltonians, can be found in Ref. [2].

Besides the more accurate first principles determination of low-lying rotational levels, our methods can also be used to study highly rotationally excited states. Of particular interest to us is the region in which the level spacing within a rotational manifold becomes comparable to a quantum of vibrational excitation. In this region one might expect our usual ideas on the separability of vibrational and rotational motion no longer to be valid. It is this problem with which we are particularly concerned at the moment. Initial calculations were performed on H_2D^+ [8] as the lightness and asymmetry of this system suggest that it will show an earlier overlap between neighbouring rotational manifolds than more conventional molecules. This was confirmed by our initial study.

We are now engaged in a systematic study of the rotational levels of this system with J values up to 30, using an accurate *ab initio* potential energy surface [22]. This should encompass the region where vibrational excitations become of lower energy than "pure" rotational excitation. It is in order to perform such calculations that the work reported here on the use of supercomputers and in particular Cray vector-processing machines has been performed. Without these machines such a study would not be feasible. We can thus say that the advent of supercomputers is opening up areas of *ab initio* molecular spectroscopy which have previously not been accessible.

Finally we should mention that the procedures developed here are well suited to machines with a highly parallel architecture. It is possible to formulate the problem for a loop of $J+p$ parallel processors with little or no shared memory, but fairly large local memory. Each processor would then be associated with a particular k value. It would:

(a) construct and diagonalise one $\mathscr{H}_k$;

Table 2. Rotational term values for D_2H^+ in cm^{-1}

	Ground state				ν_2			ν_3			ν_1	
	Expt.	Theory			Expt.	Theory		Expt.	Theory		Expt.	Theory
Level	[25]	This work	[26]	[27]	[25]	This work	[26]	[25]	This work	[26]	[a]	This work
1_{01}	34.91	34.90	34.82	34.99	30.36	30.38	30.3	40.17	40.08	40.2	34.51	34.52
1_{11}	49.26	49.25	49.15	49.38	45.93	45.92	45.9	50.27	50.22	50.2	48.34	48.34
1_{10}	57.98	57.98	57.85	57.12	58.86	58.87	58.8	57.84	57.79	57.9	56.95	56.96
2_{02}	101.72	101.67	101.48	101.93	86.94	86.98	87.0	115.63	115.45	115.5	100.57	100.53
2_{12}	110.25	110.23	109.99	110.52	94.75	94.88	94.6	124.37	124.09	124.5	108.71	108.70
2_{11}	136.38	136.31	136.02	136.66	131.75	131.71	131.6	146.73	146.55	146.5	134.48	134.43
2_{21}	179.15	179.14	178.77	179.66	177.44	177.55	177.1	176.25	176.16	176.2	175.69	175.67
2_{20}	182.06	182.03	181.66	182.55	181.40	181.48	181.1	179.15	179.08	178.9	178.61	178.57
3_{03}	196.09	196.02	195.61	196.54	165.33	165.44	165.3	219.16	218.83	219.7	193.82	193.76
3_{13}	200.04	199.96	199.63	200.50	168.33	168.47	168.8	228.31	227.89	228.1	197.55	197.48
3_{12}	251.30	251.19	250.64	251.85	237.61	237.55	237.4	272.56	272.25	272.6	248.08	247.99
3_{22}	283.32	283.24	282.68	284.05	268.20	268.29	268.0	311.06	310.46	310.6	278.82	278.73
3_{21}		295.95	295.31	296.79	284.87	284.91	284.4	319.08	318.58	318.8	291.49	291.40
3_{31}		377.06	376.29	378.27	371.56	371.93	371.0		367.64	367.2	396.59	369.51
3_{30}		377.69	376.91	378.90		366.93	365.8		368.42	368.2	370.22	370.16
4_{04}		315.62	315.20		265.26	265.39	266.4		346.70	347.0	312.11	311.98
4_{14}	317.25	317.14	316.50		266.22	266.39	266.8	361.43	360.78	362.4	313.51	313.40
4_{13}	399.06	398.88	398.11			371.71	371.9	430.17	429.76	429.8		393.88
4_{23}	419.45	419.33	418.45		388.91	388.97	388.5	462.87	462.19	462.9	413.66	413.40
4_{22}		450.58	449.64		426.40	426.40	426.4		484.83	484.8	444.61	444.41
4_{32}		519.24	518.14			504.04	503.0		495.37	495.4		510.42
4_{31}	523.40	523.30	522.18			497.26	496.8		499.91	499.4	514.66	514.49
4_{41}		643.24	641.92			689.32	688.0		624.69	624.1		630.01
4_{40}		643.35	642.04			688.24	687.0		624.87	624.1		630.12
Band origin					1968.17	1967.90	1964.7	2078.42	2079.21	2075.1	2737.00	2737.30

[a] Inferred from Table 1 of [28] using the ν_0 levels of [25]

(b) construct one block of $\boldsymbol{O}^k$, which involves sending $\boldsymbol{c}^{J,k}$ to one neighbour and receiving $\boldsymbol{c}^{J,k+1}$ from the other;
(c) construct $\boldsymbol{w}_k$ on each iteration of the diagonalisation, see (14), exchanging $\boldsymbol{z}_{k\pm1}$ with its neighbours.

Only construction of the initial matrix elements does not fall naturally into this scheme. This step typically takes only 3% of the total CPU time.

Acknowledgement. We thank the staffs of the University of London Computer Centre and the Atlas Computing Centre at the Rutherford Appleton Laboratory for their help during the course of the work presented here.

References

1. Watson JKG, Foster SC, McKellar ARW, Bernath P, Amano T, Pan FS, Crofton MW, Altman RS, Oka T (1984) Can J Phys 62:1875
2. Miller S, Tennyson J: J Mol Spectrosc, in press
3. Tennyson J, Farantos SC (1984) Chem Phys Letts 109:160; Farantos SC, Tennyson J (1985) J Chem Phys 82:800
4. Tennyson J, Farantos SC (1985) Chem Phys 93:237
5. Tennyson J (1985) Mol Phys 55:463
6. Tennyson J, Brocks G, Farantos SC (1986) Chem Phys 104:399; Brocks G: Chem Phys, in press
7. Bacic Z, Light JC (1986) J Chem Phys 85:4594; Basic Z, Light JC (1987) J Chem Phys 86:3065
8. Tennyson J, Sutcliffe BT (1986) Mol Phys 58:1067
9. Sutcliffe BT, Tennyson J: J Chem Soc Faraday Trans 2, in press
10. Sutcliffe BT, Tennyson J (1986) Mol Phys 58:1053
11. Tennyson J (1986) Comput Phys Rep 4:1
12. Tennyson J (1986) Comput Phys Commun 42:257
13. Carter S, Handy NC (1986) Mol Phys 57:175
14. Subroutine EIGSFM, Garbow BS, Boyle JM, Dongarram JJ, Moler CB (1977) Matrix eigensystems routines – EISPACK guide extension, Lect Notes Comput Sci 51. Linear Systems External User Documentation, Cray Research, Minneapolis
15. Tennyson J (1985) Comput Phys Commun 36:39
16. Tennyson J (1984) Comput Phys Commun 32:109
17. Subroutines BANDR and BISECT [14]
18. Nikolai PJ (1979) ACM Trans Math Software 5:118
19. F02FJF, NAG Fortran Library Manual, Mark 11, vol. 4, 1983
20. Saunders VR: Subroutine MXMB (private communication)
21. Tennyson J, Farantos SC: to be published
22. Meyer W, Botschwina P, Burton PG (1986) J Chem Phys 84:891
23. Tennyson J, Sutcliffe BT (1986) J Chem Soc Faraday Trans 2 82:1151
24. Pfeiffer R, Child MS Mol Phys (1987) Mol Phys 60:1367
25. Foster SC, McKellar ARW, Watson JKG (1986) J Chem Phys 85:664
26. Tennyson J, Sutcliffe BT (1985) Mol Phys 56:1175
27. Carney GD (1980) Chem Phys 54:163
28. Lubic KG, Amano T (1984) Can J Phys 62:1886